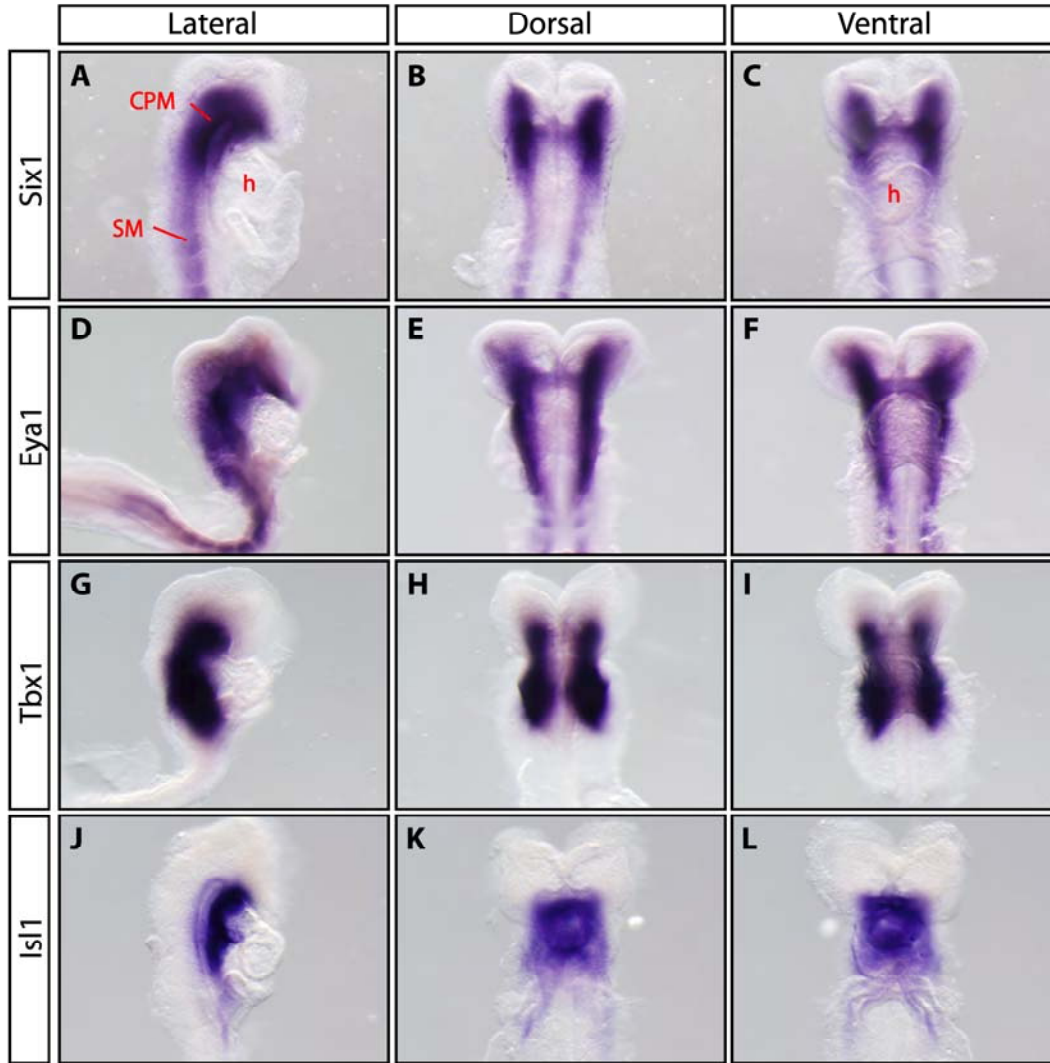


**Figure S1. *Six1* and *Eya1* control craniofacial morphogenesis.**

(A-F) Alizarin red (bone) and alcian blue (cartilage) staining of newborn *Six1/Eya1* compound mutants reveal abnormal facial structures including hypoplastic frontal nasal bones (FN, arrow head), small jawbones (\*) and ear bones as well as cleft palate (panel J). These phenotypes are similar to those seen in *Fgf8* deficient animals (Frank et al 2002). md, mandible; IE, inner ear; red, bone; blue, cartilage.

(G-N) MF20 immunohistochemical staining (red) of skeletal muscle demonstrates hypoplastic branchiomeric skeletal muscles including the first arch derived mylohyoid (Myl), digastric (Dig) and second arch derived muscles of facial expression (F) of e17.5 mutants. In addition to the branchiomeric muscle defect, which is similar to the reported *Tbx1*<sup>-/-</sup> mutants phenotype (Kelly et al., 2004), *Six1* and *Eya1* are also expressed in and required for tongue (T) muscle development as we reported previously (Li et al., 2003) (L and N). The extraocular muscles (EOM) were also hypoplastic, while masseter (Mas) muscle seemed to be less affected. Arrowhead, cleft palate; Blue, DAPI nuclear counter stain; Asterisk, hypoplastic digastricus and mylohyoid.



**Figure S2. Whole mount *in situ* hybridization of *Six1*, *Eya1*, *Tbx1* and *Isl1* in wild type e8.5 embryos.**

Lateral, dorsal and ventral views are shown to compare the expression patterns.

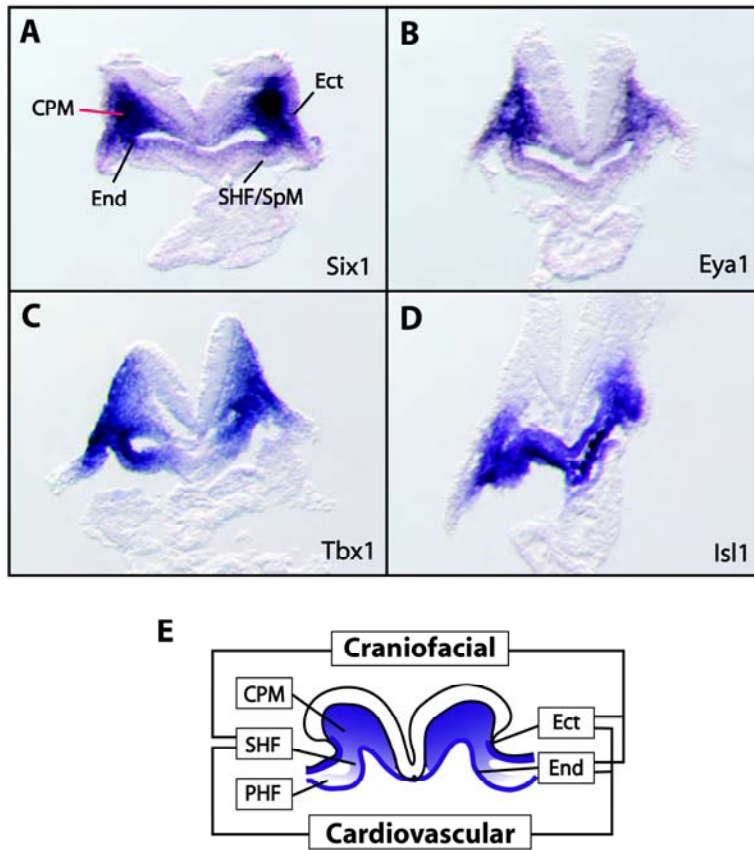


**Figure S3. *Six1*, *Eya1*, *Tbx1* and *Isl1* have partially overlapping expression patterns.**

(A-D) Transverse sections of stained embryos shown in Figure S2. *Six1* and *Eya1* exhibit a lateral-to-medial gradient expression pattern in the cephalic mesoderm with strong expression in cranial paraxial mesoderm (CPM) but much weaker expression in the second heart field (SHF)/splanchnic mesoderm (SpM). *Tbx1* and *Isl1* are strongly expressed in the SHF/SpM. All four genes are expressed at varying levels and locations in the ectoderm (Ect) and endoderm (End).

(E) Schematic cartoon displaying *Six1* and *Eya1* expression (purple) in the cephalic mesoderm, pharyngeal ectoderm and endoderm.

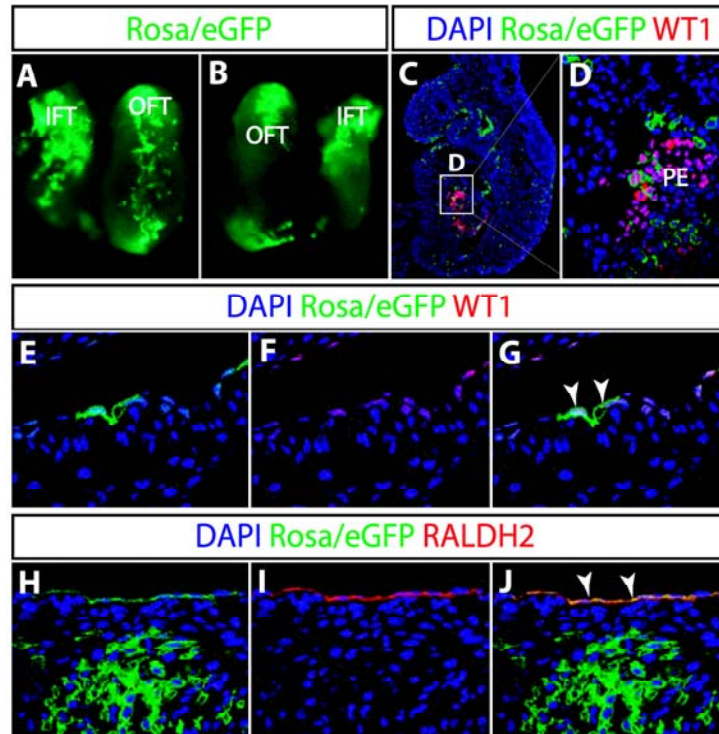


**Figure S4. *Six1* is expressed in the SHF and epicardial progenitors.**

(A-B) whole mouse dorsal-right (A) and ventral-left (B) view of the looped heart from e9.0 *Six1*<sup>Cre/hpAP</sup>;*R26R*<sup>mTmG</sup> double heterozygous embryos. eGFP<sup>+</sup> cells in the *Six1* lineage are located in inflow and outflow tracts and the looping heart tube. A similar image is shown in Figure 2F.

(C-D) eGFP colocalizes with WT1 in epicardial progenitors at e9.5; sagittal section. PE, proepicardium.

(E-J) eGFP colocalizes with WT1 (arrowheads in merged photo pane | G) and RALDH2 (arrowheads in merged photo panel J) in epicardial cells at e17.5.

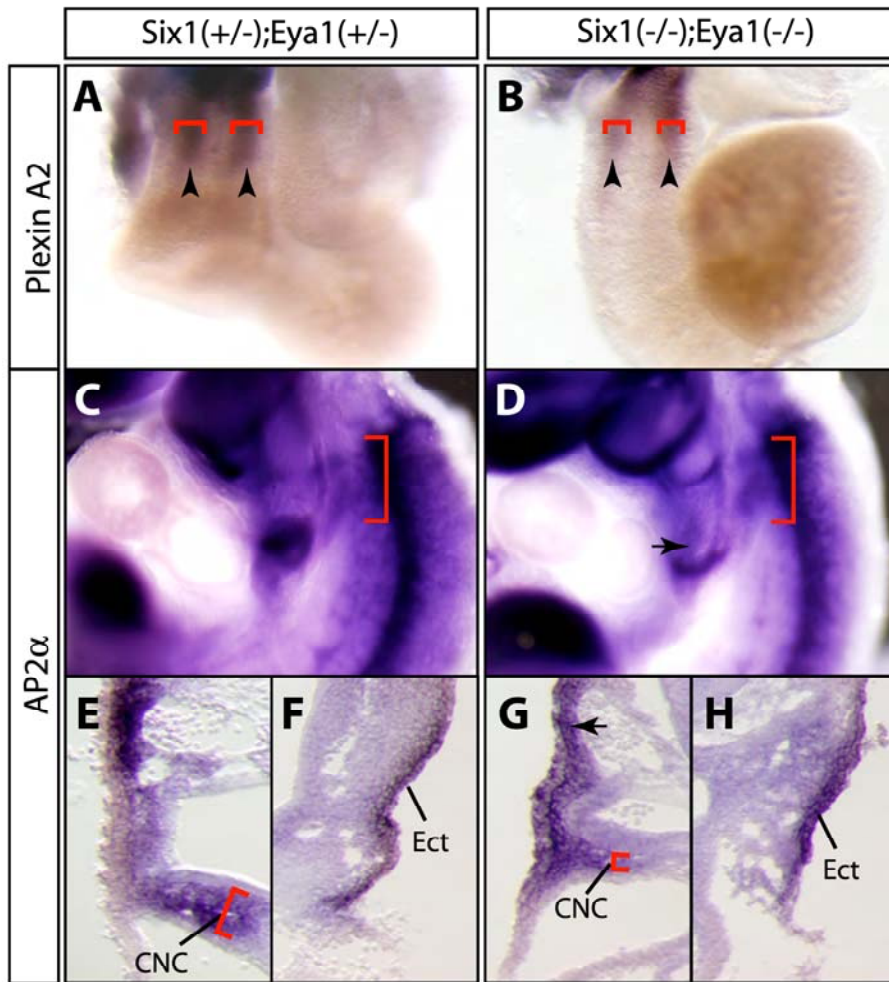


**Figure S5. Reduced expression of the cardiac neural crest cell markers.**

(A-B) Whole mount *in situ* hybridization of e11.5 embryos indicates that *Plexin A2* is strongly expressed in the prongs of CNC invading the distal cardiac outflow tract cushions (arrowheads) of a double heterozygous control and decreased in a *Six1/Eya1* double null mutant (B).

(C-D) Whole mount *in situ* hybridization indicates *AP2α* expression in cardiac neural crest and the pharyngeal ectoderm (e10.5). Brackets indicate staining of migratory cardiac neural crest. The staining in the caudal pharynx is decreased (arrow, D)

(E-H) Transverse histological sections of embryos shown in C and D indicate fewer *AP2α* stained CNCs in the mutant pharyngeal arch (G), which is consistent with the observation of increased apoptosis in the mutant (Figures 3F and I). Ectodermal *AP2α* expression appears unaffected (H).

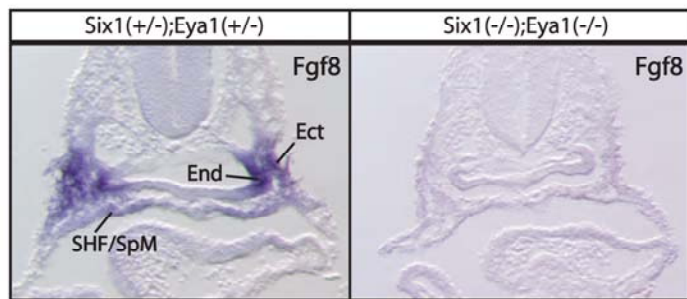


**Figure S6. *Fgf8* expression is reduced.**

Histological sections of embryos shown in Figure 4A and D indicate that *Fgf8* expression in pharyngeal ectoderm (Ect), endoderm (End) and the second heart field (SHF)/splanchnic mesoderm (SpM) are reduced in *Six1/Eya1* double null mutant.

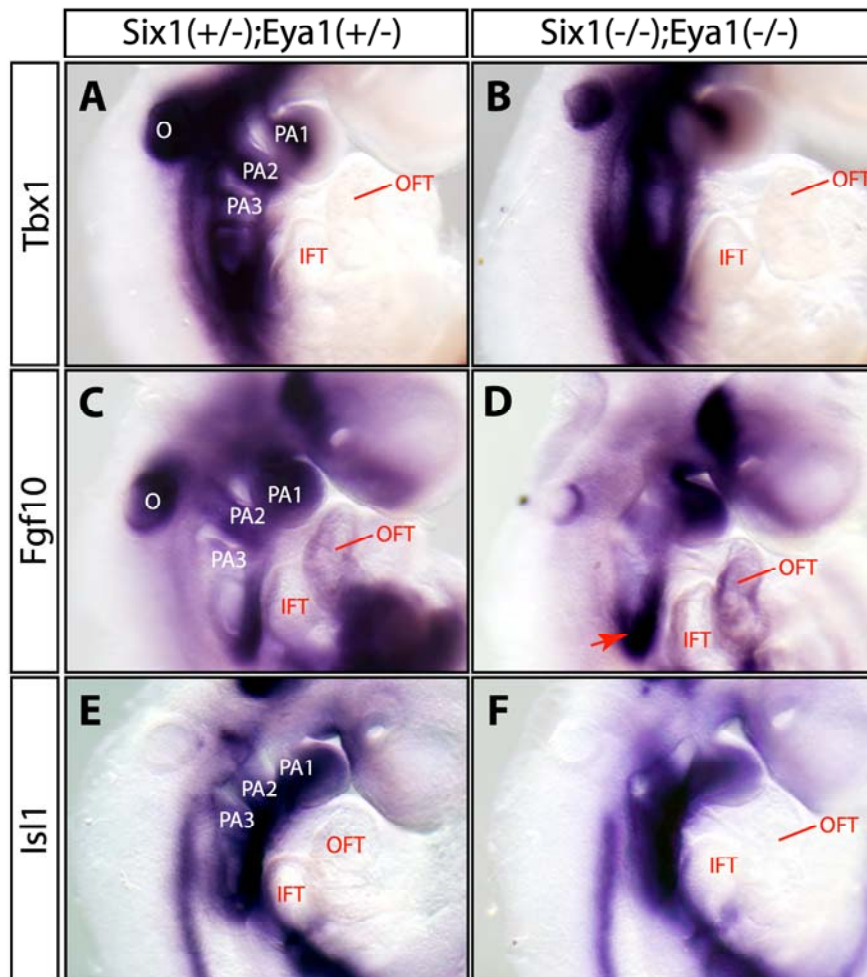


**Figure S7. Cardiac progenitors are specified in the absence of *Six1* and *Eya1*.**

Whole mount RNA *in situ* hybridization of control (A, C and E) and double null mutants (B, D and F) using *Tbx1*, *Fgf10* and *Isl1* specific probes. Expression of these SHF cardiac progenitor markers is maintained although the caudal pharynx is unsegmented in the mutants. *Fgf10* is decreased in the otocyst, but slightly increased in the OFT and caudal pharyngeal region (arrow).

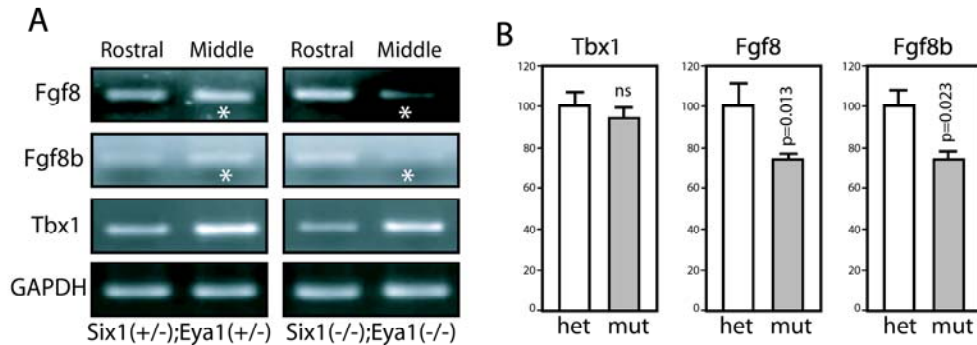


**Figure S8. Quantitative PCR analyses of the gene expression levels.**

(A) e9.5 embryos were divided into three regions: rostral (rostral of the first pharyngeal arch), middle (the pharyngeal arch apparatus and heart) and caudal (caudal to the cardiac inflow tract). Expression level of *Tbx1* and *Fgf8* (both total and isoform b) were analyzed using reverse transcription polymerase chain reaction (RT-PCR) and agarose gel electrophoresis. *GAPDH* was used as an internal control. Asterisks denote decreased *Fgf8* and *Fgf8b* transcripts detected in the pharyngeal arch/heart containing middle region. *Tbx1* expression had normal expression levels in the rostral and middle regions of mutants.

(B) Quantitative RT-PCR analyses of relative gene expression levels from the middle region (pharyngeal arch apparatus and heart) of heterozygous (het) and *Six1/Eya1* double null mutants (mut). The wildtype gene expression level compared to *GAPDH* internal control is designated as 100%. While *Tbx1* expression appears normal, total *Fgf8* transcripts and *Fgf8b*-specific isoform are decreased in the *Six1/Eya1* double null mutants (mut). Student *t*-test, n=3; ns, not significant.



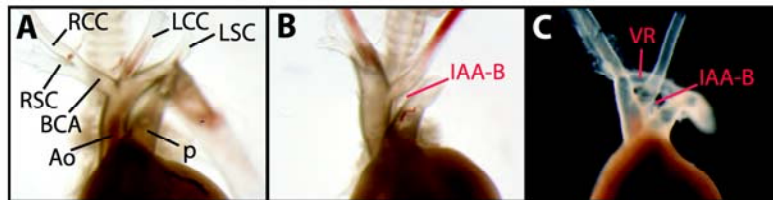


**Figure S9. *Six1* and *Fgf8* are in the same genetic pathway.**

(A-C) Newborn *Six1*<sup>Cre/-</sup>;*Fgf8*<sup>fl/+</sup> compound mutants exhibit interrupted aortic arch-type B (IAA-B, panels B and C) and vascular ring (VR, panel C). See Figure 1 legend for abbreviations.

**Table s1. Features of del22q11 patients and mouse models**

	DGS <sup>1-3</sup>	Six1/Eya1 <sup>4-6</sup>	Tbx1 <sup>7, 8</sup>	Fgf8 <sup>9-12</sup>	CrkL <sup>13-15</sup>
<b>Cardiac anomalies</b>	49-83%	+	+	+	+
<b>Craniofacial anomalies</b>	69-100%	+	+	+	+
<b>Thymus anomalies</b>	>28%	+	+	+	+
<b>Parathyroid anomalies</b>	17-60%	+	+	+	+
<b>Renal anomalies</b>	36-37%	+	NR	+	NR
<b>Growth hormone deficiency</b>	4%	+	NR	+	NR
<b>Behavior or psychiatric disorders</b>	9-45%	NR	+	NR	NR

References: (1) Kobrynski and Sullivan 2007; (2) Lindsay 2001; (3) Botto et al, 2003; (4) this study; (5) Li et al., 2003; (6) Zou et al., 2006; (7) Jerome et al., 2001; (8) Paylor et al., 2006; (9) Frank et al., 2002; (10) Abu-Issa et al., 2002; (11) Grieshammer et al., 2005; (12) Perantoni et al., 2005; (13) Guris et al., 2001; (14) Guris et al., 2006; (15) Moon et al., 2006. NR, no report.